CELL STRUCTURE AND FUNCTION 32: 29–40 (2007)

Quantitative Analysis of Cortical Actin Filaments during Polar Body Formation in Starfish Oocytes

Yukihisa Hamaguchi[1]*, Taketoshi Numata[1], and Setsuko K. Satoh[1]

[1]*Department of Bioengineering, Graduate School of Bioscience and Biotechnology, Tokyo Institute of Technology, O-okayama, Meguro-ku, Tokyo 152-8551, Japan*

ABSTRACT. **Polar body formation is an extremely unequal cell division. In order to understand the mechanism of polar body formation, morphological changes at the animal pole were investigated in living oocytes of the starfish, *Asterina pectinifera,* and the amounts of cortical actin filaments were quantitatively estimated after staining the maturing oocytes with fluorescently-labeled phallotoxins using a computer and image-processing software. Formation of a bulge, which is presumed to become a polar body, and the anaphase separation of chromosomes occurred simultaneously. When the bulge became large, one group of chromatids moved into the bulge. The dividing furrow then formed and finally a polar body formed. Just at the time of bulge formation, the intensity of the fluorescence produced by the actin filaments at the top of the animal pole began to decrease, and subsequently the intensity at the top fell to half of the original value. On the other hand, the fluorescence intensity at the base of the bulge increased gradually. This actin accumulation at the base created a dividing furrow around the top of the animal pole as the bulge grew. Even when the polar body formation was inhibited mechanically, a similar pattern of actin deficiency and accumulation in the cortex near the animal pole was observed. This indicates that such regulation of filamentous actin can take place without bulging. Therefore, polar body formation is initiated by the bulging of the cortex weakened by actin deficiency and followed by contraction of the base of the bulge reinforced by actin accumulation.**

Key words: cortical actin/dividing furrow/micromanipulation/polar body/starfish oocyte

Introduction

Polar body formation is recognized as an extremely unequal division in the oogenesis of multicellular animals. In unequal division, a furrow forms on the cortex at different distances from the two centrosomes. On the other hand, Rappaport (1961) clearly demonstrated that the furrow forms in the middle between two centrosomes in an equal division using sea urchin eggs. It is thus of pertinent interest to investigate whether polar body formation is an extraordinary cytokinesis or such normal cytokinesis as is simply explained with the contraction of a contractile ring at the equator.

*To whom correspondence should be addressed: Department of Bioengineering, Graduate School of Bioscience and Biotechnology, Tokyo Institute of Technology, O-okayama, Meguro-ku, Tokyo 152-8551, Japan.
Tel: +81–3–5734–2244, Fax: +81–3–5734–2946
E-mail: yhamaguc@bio.titech.ac.jp

Abbreviations: 1-MeAde, 1-methyladenine; DIC, differential interference contrast; MOPS, 3-morpholinopropanesulfonic acid; DAPI, 4',6-diamidino-2-phenylindole.

In starfish oocytes, polar body formation has been investigated in detail, and has been divided into stages I to V according to the changes of cell morphology (Hamaguchi and Hiramoto, 1978). In this schema, preparatory to the formation of the polar body, the cell surface expands near the animal pole and contracts around the vegetal pole, accompanied by the movement of endoplasm from the vegetal pole toward the animal pole (stage II). With the extrusion of the polar body, the cell surface around the extruded region contracts and the surface around the vegetal pole expands (stage III). After the extrusion of the polar body, the cell surface at the animal pole expands (stage IV). Accordingly, it is concluded that the extrusion of the polar body is caused by the flow of cytoplasm into the animal polar region by internal pressure in the cell after the animal polar surface is weakened by the contraction of the ring-shaped region. However, it is doubtful whether the contraction of the ring-shaped region at the animal pole would weaken the animal polar surface. On the other hand, Rappaport and Rappaport (1985) suggested that the bulge at polar body formation may not result from local surface weakening but from

regional cytoskeletal activity. However, polar body formation was not sufficiently investigated from the viewpoint of the cytoskeleton in their report. Therefore, the mechanism of polar body formation is not yet well understood even in starfish.

Phallotoxins are known to bind to filamentous actin, and fluorescently-labeled phallotoxins are useful for investigating the existence of actin filaments (Hamaguchi and Mabuchi, 1982; Strome, 1986; Yonemura and Kinoshita, 1986; Cao and Wang, 1990; Li *et al*., 1997; Crawford *et al*., 1998; Pielak *et al*., 2004, 2005). Using fluorescently-labeled phallotoxins, quantitative analysis of the actin amounts by dissecting the cortex from the total cell has recently been applied to understand the dynamic changes in the cortical actin (Satoh and Hamaguchi, 2000). This method is more useful than the methods where anti-actin antibody and fluorescently-labeled actin are used to investigate actin distribution in living and fixed cells (Byers and Fujiwara, 1982; Hamaguchi and Mabuchi, 1988) because these latter methods not only visualize filamentous actin but also globular monomeric actin.

In the present study, in order to understand the mechanism of polar body formation, morphological changes at the animal pole were investigated in living oocytes of the starfish, *Asterina pectinifera,* and the precise distribution of actin filaments in the cortex was also estimated quantitatively by means of digital image processing of the maturing oocytes stained with fluorescently-labeled phallotoxins. Furthermore, during the inhibition of the formation of the first polar body, the distribution of actin filaments in the oocyte cortex was investigated. Finally, the role of actin filaments during polar body formation is discussed.

Materials and Methods

Biological materials

Oocytes were obtained from ovaries of the starfish, *Asterina pectinifera*, and washed in Ca-free sea water (Ca-free Jamarin U, Jamarin Lab., Osaka, Japan) to remove follicle cells as reported previously (Saiki and Hamaguchi, 1998). They were treated with 2 μM 1-methyladenine (1-MeAde, Sigma, St. Louis, MO) in sea water to induce meiotic divisions, in accordance with the method reported by Kanatani (1969). Maturing oocytes were inseminated 35 min after the addition of 1-MeAde to elevate the fertilization envelope and to facilitate the observation of polar body formation.

In some experiments, fertilized eggs were deprived of both the fertilization envelope and jelly coat by being treated for 1 min with 1 M glycine solution shortly after insemination (Rappaport and Rappaport, 1985) and incubated in Ca-free sea water (Ca-free Jamarin-U, Jamarin Lab., Osaka) at 20°C.

Inhibition of polar body formation

Two types of inhibition experiments were carried out. Many inhibited oocytes were obtained simultaneously by one of the inhibition experiments and images of the cortex taken perpendicularly to the optical axis were observed, but a single inhibitory oocyte was obtained using micromanipulation by the other experiment and an image of the cortex parallel to the axis was observed.

In the former inhibition experiment, when many oocytes were compressed in a trough at a thickness of 100 μm, polar body formation did not occur in the oocytes when the animal pole faced the coverslip of the trough; that is, the oocytes were positioned with the animal-vegetal axis parallel to the optical axis of the microscope. On the other hand, even in such compressed oocytes, which were used as controls, when the animal pole faced the orifice of the trough, i.e., when the animal-vegetal axis of these oocytes was placed perpendicular to the optical axis, polar body formation occurred. These oocytes were fixed for 30 min at an appropriate time after 1-MeAde treatment and stained with BODIPY FL-phallacidin for 12 hr instead of 30 min.

In the latter inhibition experiment, among the oocytes which were placed in the trough at a thickness of 100 μm, the oocytes whose animal pole faced the orifice of the trough and in which polar body formation was presumed to occur were used. Using such compressed oocytes, micromanipulation was carried out using a micromanipulator (MO-102R, Narishige Scientific Instrument Lab., Tokyo, Japan) as follows. A thin piece of coverslip was cut and attached to a micropipette which was made with a needle puller from a glass capillary with 1-mm outer diameter. In order to inhibit polar body formation, the edge of the coverslip was pushed for 15 min against the bulging region of the maturing oocyte in the trough until the surface of the oocyte attached to the edge reached a diameter of 60 μm. To observe actin distribution, the oocyte was fixed and labeled with BODIPY FL-phallacidin.

Fluorescence labeling

At an appropriate time after nuclear envelope breakdown the fertilized eggs were fixed for 30 min with glucose F-buffer supplemented with 3.0% formaldehyde according to Mabuchi (1994) with a slight modification. Glucose F-buffer contained 0.1 M KCl, 2 mM $MgCl_2$, 1 mM EGTA, 10 mM MOPS (3-morpholinopropanesulfonic acid, pH 7.4), and 0.5 M glucose. The eggs were stained for 30 min with rhodamine-phalloidin or BODIPY FL-phallacidin for actin filament observation and DAPI (4',6-diamidino-2-phenylindole) for 10 min for chromosome observation. Rhodamine-phalloidin and BODIPY FL-phallacidin solutions dissolved in methanol (Molecular Probes, Inc., Eugene, Oregon) were diluted 150 times in the glycerol F-buffer supplemented with 1% β-mercaptoethanol, and DAPI was dissolved at 0.5 μM in the buffer. Glycerol F-buffer contained the same components as glucose F-buffer, with 0.5 M glycerol added instead of 0.5 M glucose.

Observation

Living oocytes were observed mainly with a differential interference contrast (DIC) and polarization microscope (TMD, Microphot, or Optiphot, Nikon, Tokyo, Japan). The image was taken on 35-mm film or by video-enhanced microscopy, which was carried out using a video camera (WV1550, Panasonic, Tokyo) and an image processor (Image Sigma-II, Nippon Avionics Co. Ltd., Tokyo).

In order to observe chromosome movement in a living oocyte by DIC microscopy, a solution containing fructooligosaccharides (Wako Pure Chemical Industries, Ltd., Tokyo) whose refractive index was near that of the oocytes was perfused in the trough, and the oocyte was then cultured in this solution.

The fixed and stained eggs were observed with a fluorescence microscope equipped with an objective of Fluor 10x (NA=0.5) and an epi-illumination apparatus, and their images were taken with a CCD camera (C2400-75I, Hamamatsu Photonics, Hamamatsu) using a computer through an image processor (Argus 20, Hamamatsu Photonics), as shown in Fig. 4 and Fig. 5. The results in Fig. 11 were obtained with a fluorescence microscope equipped with a UV-F 40x oil immersion objective (NA=1.30), the other results were obtained with this microscope supplemented by a confocal fluorescence apparatus (InSIGHTplus, Meridian Instruments Inc., Okemo, Michigan), and their images were taken with a CCD camera (MicroImager, Xillix Technologies Corp., Richmond, BC, Canada).

Quantitative analysis of cortical actin

The amount of actin filament was estimated from the fluorescence intensity of the oocyte stained with fluorescently-labeled phallotoxins. Quantitative analysis of fluorescence intensity in the cortex of the oocyte was carried out as described in Satoh and Hamaguchi (2000) and described briefly. Densitometric analyses were performed on a Power Macintosh 7500 computer using the public domain NIH Image software written by Wayne Rasband at the National Institutes of Health as described in Method I (Fig. 1) and Method II (Fig. 2). Fluorescence digital images of the oocytes had two-dimensional arrays of pixels ranging in value from 0 to 255. One pixel in the fluorescence image corresponded to 0.38 μm in length at low magnification and 0.23 μm at high magnification.

Method I: As schematically shown in Fig. 1a, the mean values of fluorescence intensity/pixel in rectangular regions of 5×20 pixels (1.9×7.7 μm) on the polar (P) and equatorial (E) cortices and in a region of the same area outside the oocyte as background (B) were measured at low magnification. The fluorescence ratio (R) of the equatorial cortex to the polar cortex was calculated according to the equation (1).

$$R=(P–B)/(E–B) \quad (1)$$

At high magnification, an image of the whole oocyte could not be obtained. As shown in Fig. 1b, the mean values of fluorescence intensity/pixel in the circular regions of 6 pixels (1.4 μm) on the animal pole (P) cortex and control (E) cortices, which were then 50 μm distant from the animal pole instead of the equatorial cortex, and in a region (B) of the same area outside the oocyte as background were measured at high magnification. The fluorescence ratio (R) of the equatorial cortex to the control cortex was calculated according to equation (1).

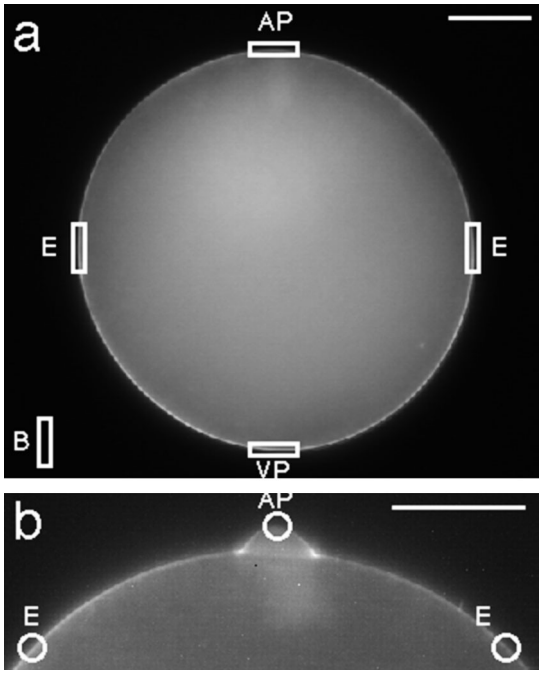

Fig. 1. Fluorescence images representing cortical actin measurement by Method I. Image (a) was taken at low magnification. Bar=50 μm. Open rectangles indicate measured regions; i.e., the animal pole or vegetal pole and the reference equatorial cortices, but they are not the real size of the measured area, where the mean light intensity/pixel was measured. Image (b) was taken at high magnification. Bar=20 μm. Open circles indicate measured regions; i.e., the animal pole and the reference cortices, which are the cortices at 50 μm far from the animal pole in this case, where the mean light intensity/pixel was measured. The upper side of these micrographs was set at the animal pole of the oocytes. B; background, E; equator or reference regions, AP; the animal pole, VP; the vegetal pole.

Method II: From the fluorescence image of an oocyte (Fig. 2b) stained by fluorescently-labeled phallotoxins, the contour of the oocyte was detected by using an edge function or a macro of our own making in NIH Image software. Using this contour, the cortex of the animal pole region in the oocyte at a thickness of 6 pixels (1.4 μm) at high magnification was dissected from the fluorescence image as shown in Fig. 2b. In the case of actin filament along the animal-vegetal axis, the total density in all of the one-dimensional pixels of a column of the cortical image was divided by the pixel number in the same column where the density was not zero and then in every column the mean intensity was also calculated in the same manner using a macro of our own making in NIH Image software. This mean intensity in a column corresponds to P in the equation (1). The ratio (R) was then obtained along the axis by means of calculating this mean fluorescence intensity which was divided by the mean fluorescence intensity corresponding to

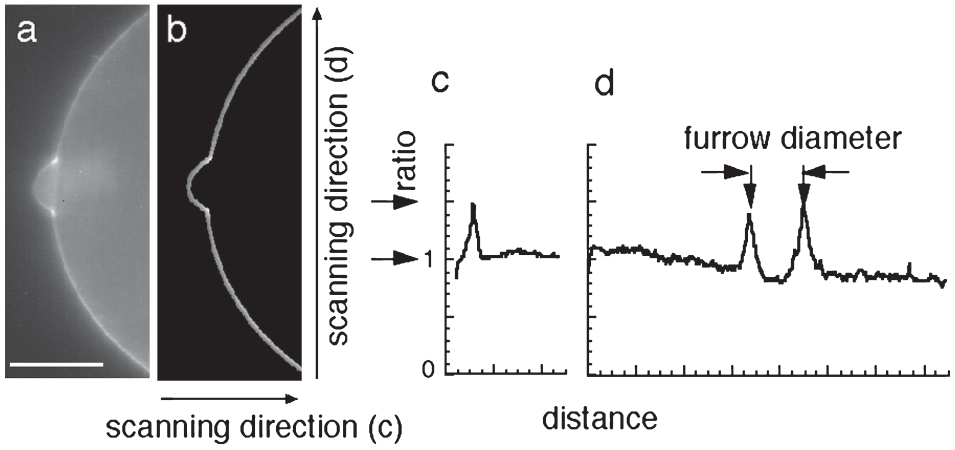

Fig. 2. Schematic representation of measuring the peak intensity and diameter of the dividing furrow in fluorescence images by Method II. In the case of measuring the peak intensity, image (b) of the cortex at the thickness of 1.4 μm was dissected from the fluorescence image (a) by computer processing and the mean light intensity/pixel was measured by scanning from the left to the right; i.e., from the animal side to vegetal side and then the maximum value of the intensity (the arrow) obtained was regarded to be the peak intensity (c). In the case of measuring the diameter of the dividing furrow, the mean intensity of the cortex of the fluorescence image (b) was measured by scanning from the bottom to top; i.e., perpendicular to the animal vegetal axis, the distance between the peak values (two arrows) was measured to be the distance of the furrow diameter (d). Bar=20 μm.

(E) in the equation (1) at the two sites which were 50 μm distant from the animal pole, followed by subtracting the background intensity (B) as shown in equation (1) (Fig. 2c). The fluorescence distribution was also calculated along a line perpendicular to the axis (Fig. 2d). In the case of actin filament along the animal-vegetal axis, one peak was obtained and the value was designated as an actin accumulation value at the furrow even if the furrow was not apparently observed by ordinary microscopy. In the case of actin filament perpendicular to the animal-vegetal axis, two peaks were obtained, and the distance between the peaks was designated as the furrow diameter. The fluorescent intensity at the peak site was obtained on the average from a cortex of 20 pixels in length.

Results

Morphological changes near the animal pole during the formation of the first polar body

Morphological changes during first polar body formation occur in whole cells: Just before polar body formation, the cell surface expands at the animal pole and contracts at the vegetal pole (stage II in Hamaguchi and Hiramoto (1978)), and the cell surface around the extruded region then contracts and the surface at the vegetal pole then expands (stage III). The diameter of the cell also changes quickly as reported by Shirai and Kanatani (1980).

However, morphological changes near the animal pole were more remarkable than those of the whole cell. As shown in Fig. 3, both the morphological changes near the animal pole and the chromosome movement were observed by DIC microscopy in some oocytes. At metaphase, chromosomes were situated at a distance of 10 μm from the animal pole in this oocyte (Fig. 3a). The chromosomes began to separate at anaphase and, simultaneously, a region of 30–40 μm in diameter at the animal pole began to bulge (Fig. 3b–c). When the bulge became prominent, one group of chromatids (peripheral chromosomes) moved into the bulge (Fig. 3f–g). After a furrow formed at the base of the bulge, the peripheral chromosomes moved to the position of the furrow and were incorporated into the forming polar body (Fig. 3h). The furrow then ingressed and constricted the equator of the mitotic apparatus for the first polar body formation (Fig. 3h–i), and finally, the furrow constricted the extruded polar body containing the chromosomes (Fig. 3j). The distances from the chord to the peripheral and the inner chromosomes were measured as the distances of the peripheral chromosomes and the inner chromosomes added to the height of the animal pole and the diameter of the bulge or the dividing furrow in an oocyte as described below (Fig. 4c). Anaphase chromosome movement was almost finished before the dividing furrow was formed, although no single nucleus either in the oocyte or in the polar body was found.

Moreover, the duration of polar body formation was only 5–7 min after the oocyte began to bulge, and polar body formation did not occur simultaneously in every oocyte. Hence, in order to compare the events in living oocytes with the cytoskeletal observations in fixed oocytes, we determined the indicator of polar body formation as follows (especially during stage III in the reference of Hamaguchi and Hiramoto, 1978). During polar body formation, because bulge height or bulge diameter is not a good indicator for comparing the stage of individual oocytes, first, in the image of the oocyte, the indicator we selected was a chord

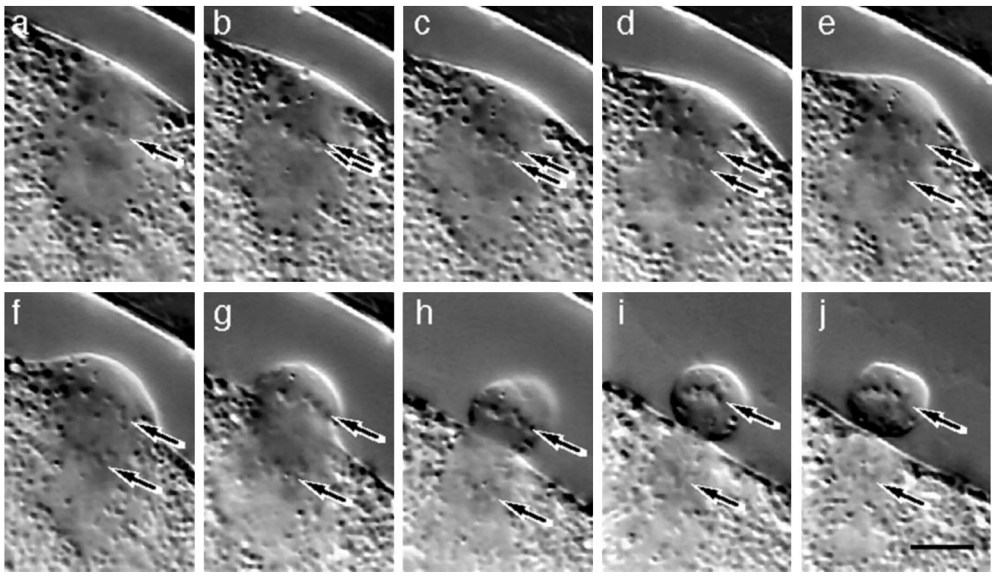

Fig. 3. Morphological changes near the animal pole and chromosome movement in a starfish oocyte during the first polar body formation at high magnification. Image (a) was taken 46 min after treatment with 1-MeAde and images (a)–(j) were taken at 40 sec intervals. The top side is the animal pole. Arrows show chromosomes. Bar=10 μm.

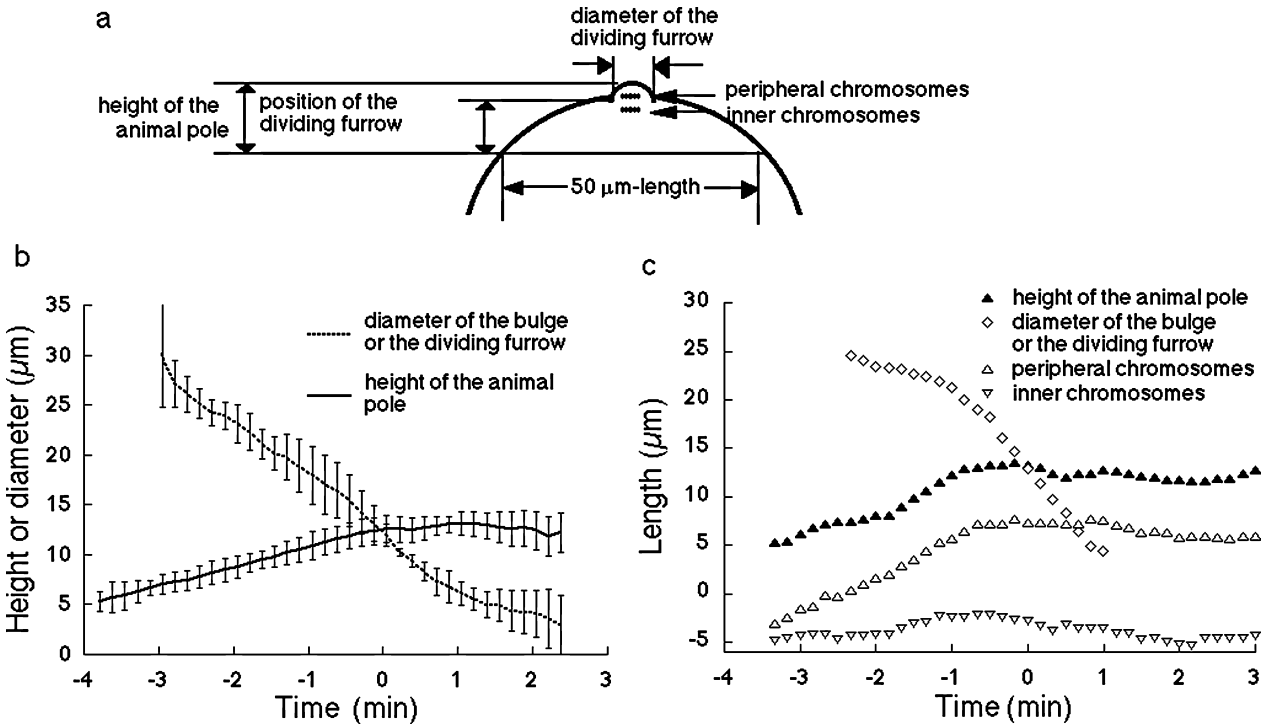

Fig. 4. Normalization of morphological changes during polar body formation. (a) Schematic representation of measured distances showing the progress of polar body formation. The indicators of the stage of polar body formation were defined as follows. The height of the animal pole is the distance measured from the animal pole to a 50 μm-length chord set perpendicularly to the animal-vegetal pole axis. The diameter of the dividing furrow was also measured. The distances of the peripheral chromosomes and the inner chromosomes were measured as the distances between the chord and the peripheral chromosomes and the inner chromosomes. (b) The height of the animal pole and the diameter of the dividing furrow were measured in living cells and averaged in 8 specimens as the time when the diameter of the dividing furrow became 12 μm was 0. (c) The height of the animal pole, the diameter of the dividing furrow, the position of the dividing furrow, and the distances of the peripheral chromosomes and the inner chromosomes were measured in an oocyte were plotted versus the same time in (b).

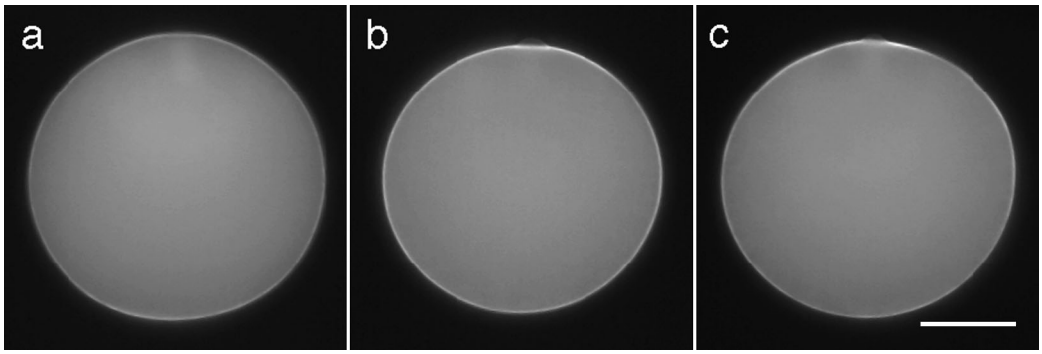

Fig. 5. Fluorescence images of starfish oocytes during polar body formation at low magnification. Images (a), (b), and (c) were taken at 54, 60, and 63 min after treatment with 1-MeAde, respectively. The top side is the animal pole. The bulge was not observed in image (a), but the fluorescence in the cortex of the bulge was slightly observed in images (b) and (c) over the brightly fluorescent cortex around the bulge at the animal pole. Bar=50 μm.

with a length of 50 μm, which was perpendicular to the animal pole, as shown in Fig. 4a. The length of 50 μm was selected because 50 μm is greater than the bulge diameter. The distance from the chord to the pole was measured as the height of the animal pole, and the diameter of the bulge or the dividing furrow was measured in an oocyte as shown in Fig. 4a. The time when the diameter of the dividing furrow decreased to 12 μm was designated as time 0 in this study (12 μm, which is also nearly equal to the diameter of a polar body and means the onset of furrowing in the case of equal cell division), and then, at –3–4 min, a bulge began to form. The mean value of the height of the animal pole increased linearly during the early process of polar body formation and then became constant in the late process as shown in Fig. 4b. Therefore, the height of the animal pole was a good indicator of polar body formation during the early process of polar body formation, although it is not a good indicator during the late process. On the other hand, although the mean value of the bulge diameter decreased linearly, its standard deviation was so large just when it was beginning to bulge as shown in Fig. 4b that the diameter was not an adequate indicator of polar body formation during the early process. However, after the furrow formed, the mean value of the diameter of the dividing furrow decreased linearly, and the diameter of the furrow was then a good indicator of polar body formation except for the early process. The time course of the increase in the height of the animal pole and the decrease in the diameter of the furrow crossed at 0 min.

Actin distribution in the cortex during polar body formation

The actin distribution in the oocyte cortex was estimated by fluorescently labeling the oocyte with rhodamine-phalloidin. Before bulge formation for the first polar body, the fluorescence intensity of the cortex at the animal and vegetal poles was relatively constant compared with that at the equator (Fig. 5). Although fluorescence was also found in the

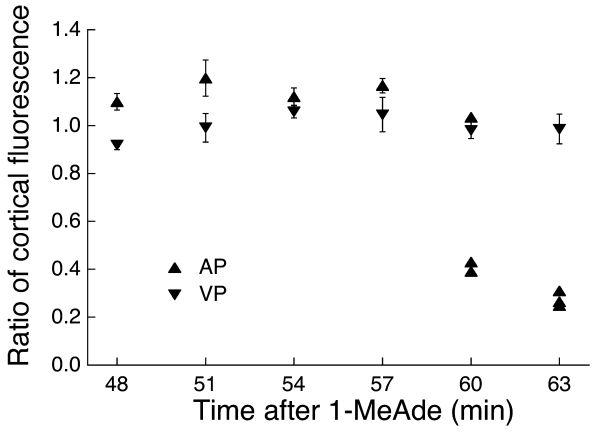

Fig. 6. Ratio of cortical fluorescence intensity at the animal pole and the vegetal pole to the equatorial cortex of the oocytes after the treatment with 1-MeAde. Fluorescence intensity at the vegetal pole was about 1.0 at 48–63 min after 1-MeAde treatment, but fluorescence intensity at the animal pole decreased at 60 and 63 min after 1-MeAde treatment in some and all oocytes, respectively, and in such oocytes the bulge was found at the animal pole. Abscissa: time after addition of 1-MeAde (min); ordinate: ratio of fluorescence intensity.

oocyte interior, especially near the mitotic apparatus, it was not investigated in this study. In each oocyte, the optical conditions were almost equal, autofluorescence was negligible, and, therefore, the fluorescence distribution is believed to reflect the distribution of the amounts of actin. The fluorescence intensity of the cortex was measured at the animal pole, vegetal pole, and equatorial cortex. We then calculated the ratio of fluorescence of an interested cortex to the equatorial cortex but not the absolute intensity of fluorescence of the cortex during polar body formation. Hence, before bulge formation, the cortical fluorescence at the animal pole was more than that at the vegetal pole, although the fluorescence ratio of the equatorial cortex to the polar cortex was almost 1 (Fig. 6). After bulge formation, the intensity of the cortex

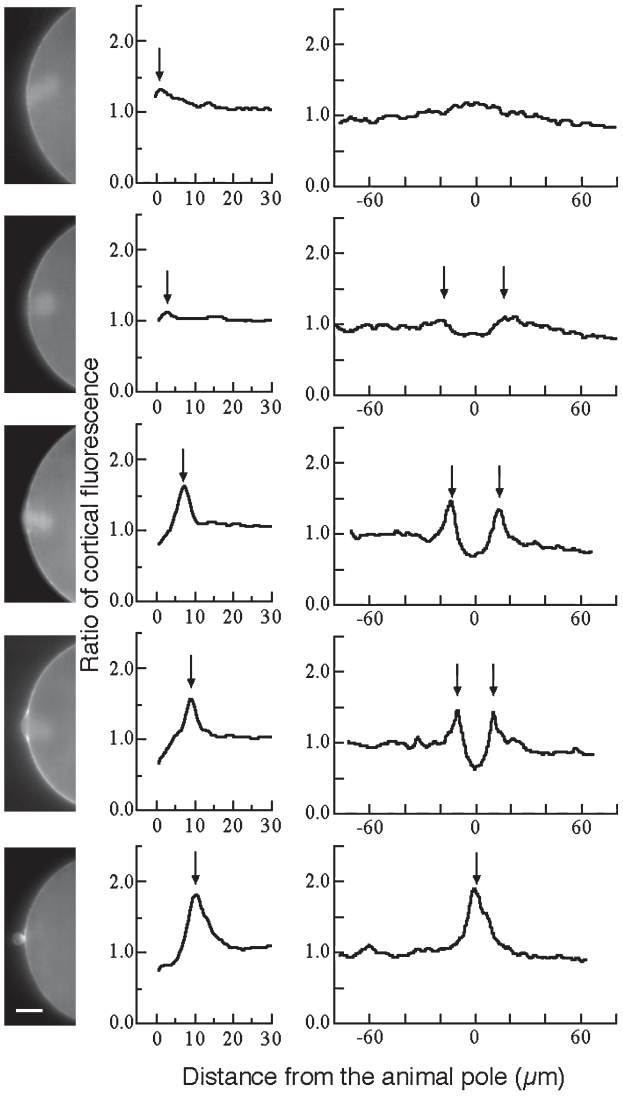

Fig. 7. Ratio of cortical fluorescence intensity measuring the diameter and peak intensity of the dividing furrow in fluorescence images. In the same row, three figures from an oocyte are represented. From the top to the bottom, the micrographs are aligned in the order of the stage of polar body formation. In the left column, the animal polar regions of maturing oocytes are shown. Bar=20 μm. In the middle column, mean light intensity/pixel measured from animal side to vegetal side is plotted. In the right column, mean light intensity/pixel measured perpendicularly to the animal-vegetal axis is plotted. Arrows indicate the peaks of light intensity.

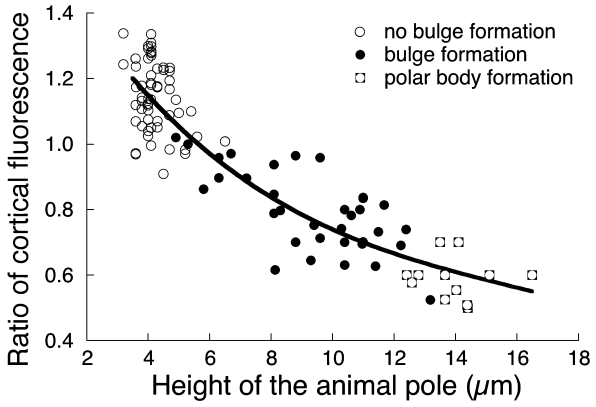

Fig. 8. Relationship between the ratio of cortical fluorescence at the animal pole and the height of the animal pole. Open circles are those of the oocytes where the bulge at the animal pole was not observed, closed circles are those of the oocytes where the bulge at the animal pole was observed, and circles in rectangles are those of the oocytes where the base of the bulge became the furrow. Abscissa: the height of the animal pole (μm). The increase in this height of the animal pole indicates progress in polar body formation as shown in Figure 4b. Ordinate: ratio of the cortical fluorescence at the animal pole to the reference cortex.

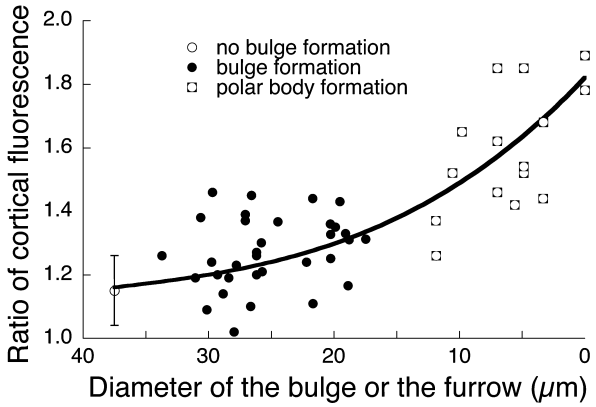

Fig. 9. Relationship between the peak fluorescence intensity at the furrow and the diameter of the bulge or furrow. Closed circles are those of the oocytes where the bulge at the animal pole was observed. Circles in rectangles are those of the oocytes where the base of the bulge became a furrow. In the oocyte where no bulge formation was observed, the mean fluorescence intensity at the animal pole is shown although the diameter of the bulge or furrow could not be determined. Abscissa: the diameter of the bulge or the furrow (μm). The decrease in this diameter of the bulge or the furrow indicates progress in polar body formation as shown in Figure 4b. Ordinate: ratio of the cortical fluorescence at the animal pole to the reference cortex.

at the animal pole suddenly decreased and the ratio of fluorescence intensity at the animal pole after bulge formation dropped to 0.4, whereas that at the vegetal pole did not change (Fig. 6).

In order to measure the actin distribution in the cortical region of the animal pole during polar body formation precisely, the fluorescently-labeled oocytes were observed with a confocal microscope. After the cortical regions were dissected from the images, the fluorescence intensity in the cortex was determined along the animal-vegetal axis and perpendicular to the axis as shown in Fig. 7. The fluorescence intensity of the cortex at the animal pole decreased proportionally to the increase in the height of the animal pole and, in the surface of the polar body, the intensity became 0.5 compared with that of the control cortex (Fig.

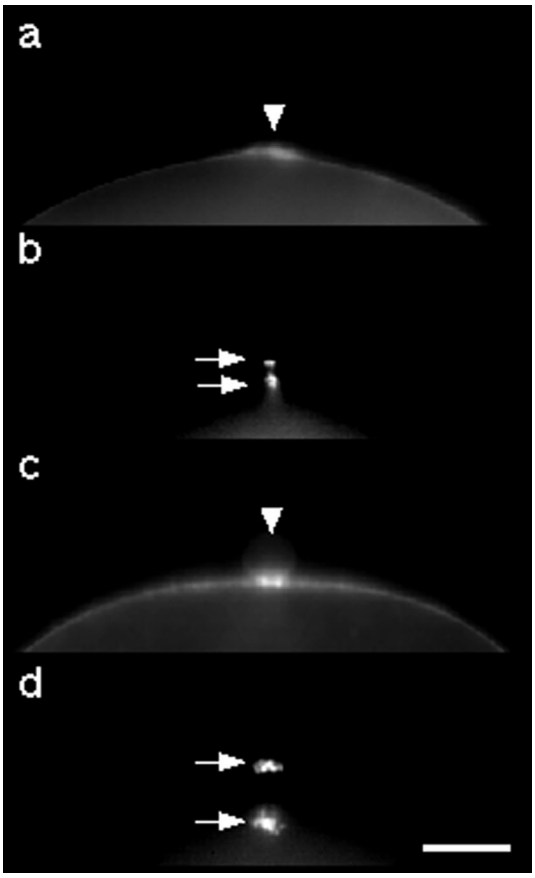

Fig. 10. Inhibition experiment of polar body formation by compressing with the edge of a small piece of coverslip attached to a micropipette. Images (a), (b) are fluorescence micrographs of the oocyte where polar body formation had been inhibited by compression by pushing a thin piece of coverslip against the cortex of the animal pole. Images (c), (d) are fluorescence micrographs of a control oocyte where the first polar body has just formed. Images (a) and (c) show actin distribution, and the arrowhead indicates the animal pole. Images (b) and (d) show chromosomes and the arrows indicate them. Bar=20 μm.

8). At the base of the bulge, actin accumulation was observed. Shortly after bulge formation, the fluorescence intensity was about 1.2 and gradually increased to 1.8-fold compared with that of the control cortex (Fig. 9). According to the analysis using living oocytes, the stage when the height of the animal pole is equal to 12 μm in Fig. 8 is the same stage as that when the diameter of the bulge or the furrow is 12 μm in Fig. 9.

Actin distribution in the oocytes when polar body formation is inhibited

In order to inhibit polar body formation, the edge of the coverslip was pushed for 15 min against the bulging region of the maturing oocyte in the trough. Fluorescence distribution is represented after fluorescence labeling in Fig. 10. Actin accumulation was observed in the cortex at the animal pole and there was a small dark area in the center of this accumulated region, which suggests that this fluorescence distribution is similar to that of a contractile ring during normal polar body formation compared with the fluorescence at the furrow in a control oocyte (Fig. 10). The diameter of the ring-like fluorescence was determined to be 5.4±1.9 μm (sample no.=5).

In order to observe fluorescence distribution in the cortex in detail, polar body formation was inhibited in the oocytes where the animal pole faced the coverslip of the trough when the oocytes were placed in the trough at a thickness of 100 μm. Fluorescence distribution parallel to the cortex but not in cross section is shown in Fig. 11. A dark region in the cortex over the chromosomes was observed, which is presumed to be the bulge. In some oocytes, actin accumulation was observed as a ring in the dark region (Fig. 11d), which is similar to a contractile ring during normal polar body formation, and this ring-like fluorescence was at a diameter of 13.7±3.7 μm (sample no.=12) near the animal pole. When the oocytes where polar body formation was inhibited were fixed at an appropriate time, the diameter of the actin-rich ring became short and then slightly long, which indicates that the ring might contract and then relax (Fig. 11g). Therefore, by inhibition of the polar body formation, actin deficiency was induced in the cortex at the animal pole in a manner similar to that in the bulge cortex of normal oocytes, and also actin accumulation in the form of a ring was induced at the cortex distant from the animal pole similar to that in the furrow in normal oocytes.

Discussion

The relationship between bulge formation and furrow formation

Remarkable morphological changes occur near the animal pole during polar body formation. In this study, these changes and chromosome movement were observed in living oocytes as shown in Fig. 3 and Fig. 4. When the chromosomes were found to be separating at the beginning of anaphase, simultaneously the cortex at the animal pole began to bulge. Two to three min after the beginning of bulge formation, a furrow formed at the base of the bulge, and finally the furrow constricted the extruded polar body. In other words, bulge formation is a phenomenon at the beginning of anaphase, while furrow formation is a phenomenon at the midstage of anaphase to telophase, which would be the same stage in equal division (Fig. 12). Longo (1972) pharmacologically dissected these two phenomena: by treating the maturing oocytes of the surf clam, *Spisula,* with cytochalasin B, a bulge formed, but a division furrow did not. Rappaport and Rappaport (1985) microsurgically dissected the two phenomena: by inserting a pair of nearly

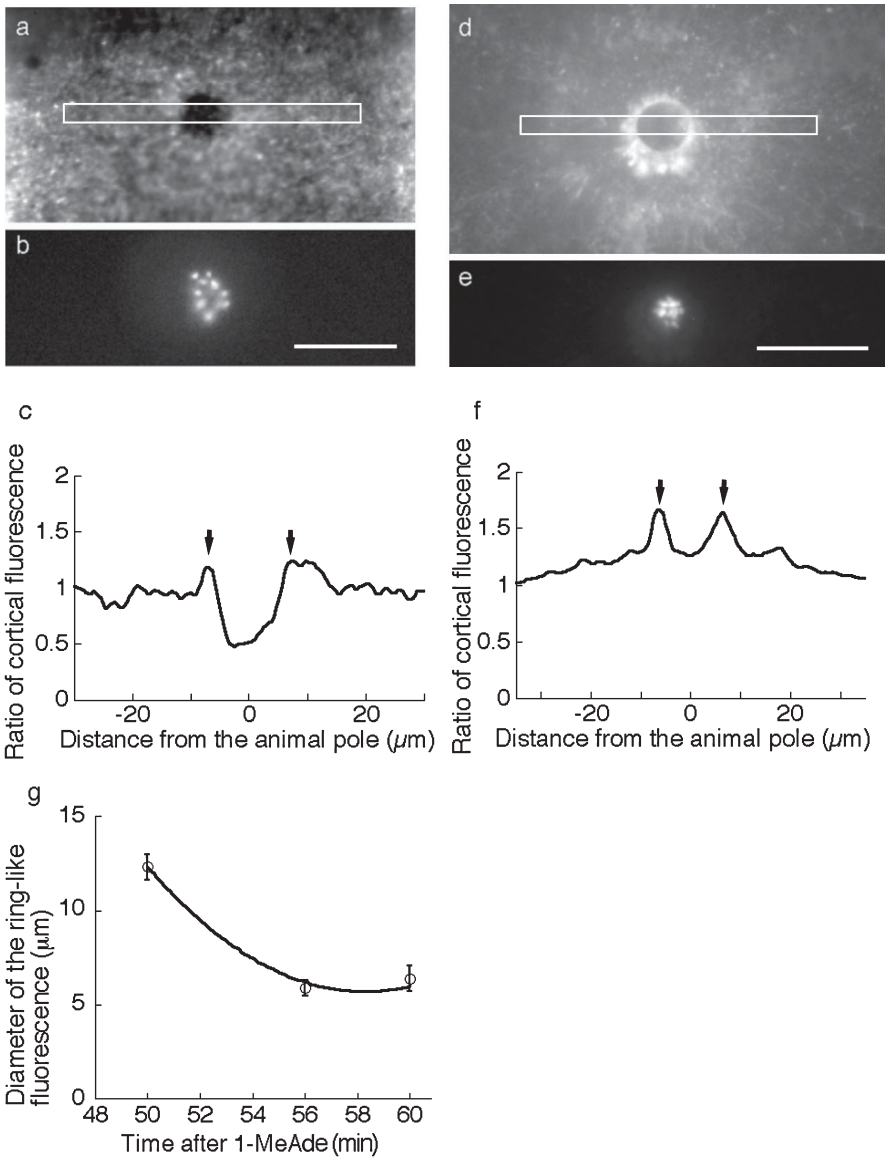

Fig. 11. Inhibition experiment of polar body formation, compressing oocytes with a pair of coverslips. Images (a), (b), (d), and (e) are fluorescence micrographs of the compressed oocyte where polar body formation has been inhibited. Polar body formation did not occur in the oocytes when the animal pole faced the coverslip of the trough at a thickness of 100 μm; i.e., the oocytes were placed with their animal-vegetal axis parallel to the optical axis of the microscope. Images (a) and (d) show actin distribution, and images (b) and (e) show chromosomes. Bar=20 μm. In (c) and (f), the mean light intensity/pixel was measured along a 0.7 μm thick strip that crossed the central region where the polar body is presumed to form, as illustrated by the open rectangle in images (a) and (d), respectively. The distance between the two maximal intensities in these figures (the distance between the two arrows) was measured as the diameter of the contractile ring-like structure in order to make the chart (g). The chart (g) shows the time course of the contractile ring-like accumulation of actin fluorescence during the inhibition of polar body formation. By this method, polar body formation was simultaneously inhibited in many oocytes by compressing the oocytes to a thickness of 100 μm and fixing them at 50, 56, 60 min after treatment with 1-MeAde. The contractile ring-like accumulation of actin fluorescence was observed at a mean diameter of 13 μm at 50 min after treatment with 1-MeAde and the mean diameter of the contractile ring-like accumulation decreased to 6 μm at 56 min after treatment with 1-MeAde.

parallel microneedles at a distance of 12 to 25 μm from each other into the cortex of the presumptive polar body region of the maturing oocytes of the starfishes, *Pisaster* and *Asterias,* the paired microneedles prevented the presumptive contractile ring from constricting a bulge into a polar body, although a bulge formed. Therefore, bulge formation and furrow formation are caused by temporally different mechanisms.

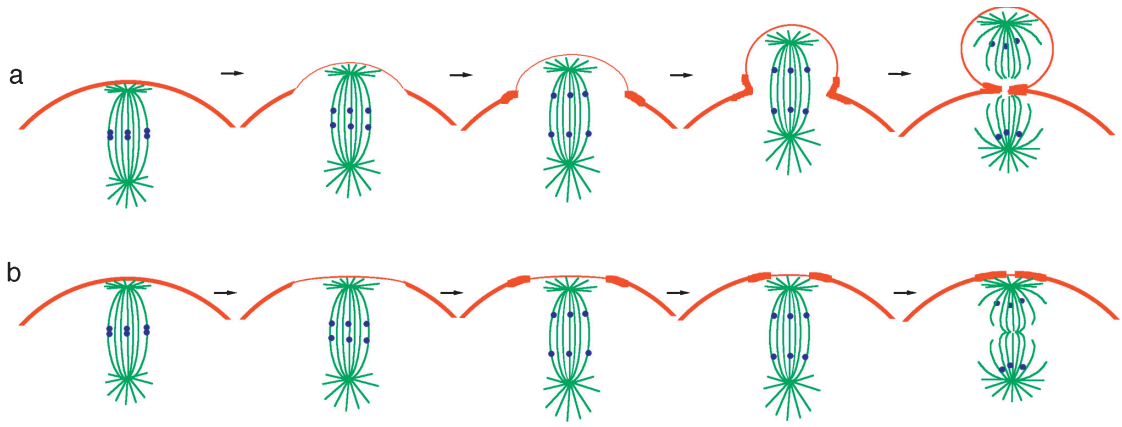

Fig. 12. Schematic representation of actin distribution in the cortex and morphological changes in the oocyte during polar body formation. Actin levels in the cortex are represented by the varying thicknesses of the red line of the cortex. The mitotic apparatus is also shown in this figure because the cortical changes occur simultaneously with the anaphase chromosome movement. Chromosomes are shown by filled blue circles and microtubules are green lines. (a) Normal polar body formation: Shortly after the onset of anaphase, actin in the cortex near the animal pole decreases and simultaneously a bulge appears around the pole. Actin in the cortex then increases only at the base of the bulge. The base of the bulge contracts with increase in bulge height, and finally the bulge changes to a polar body. During contraction, actin in the cortex of the bulge or the polar body decreases, while actin in the cortex of the base of the bulge or the polar body increases. (b) Inhibition of polar body formation: Shortly after the onset of anaphase, actin in the cortex near the animal pole decreases without bulging, while actin in the cortex is found only at the edge of the actin-decreased area near the animal pole. The diameter of this latter area decreases as the edge of the circle contracts and as the meiotic stage progresses.

Cortical actin distribution

In the present study, we estimated the amounts of the cortical actin filaments quantitatively by means of digital image processing of the dividing oocyte stained with fluorescently-labeled phallotoxins. Digital image processing is very useful to estimate the distribution of some molecules as reported by the present authors and some other investigators (Satoh *et al*., 1996; Yumura and Fukui, 1998; Satoh and Hamaguchi, 2000; Robinson *et al*., 2002). Because the duration of polar body formation is so short and because it does not occur simultaneously in every oocyte, it is difficult to compare the precise process of polar body formation in living cells to that in fixed ones. In order to compare them, the height of the animal pole and the diameter of the furrow were used as indicators of the early and late stage of polar body formation, respectively. Heil-Chapdelaine and Otto (1996) investigated the cortical actin of oocytes of the starfish, *Asterina,* during the maturation process using rhodamine-phalloidin, but they did not analyze local change in cortical actin.

The fluorescence intensity of the cortex at the animal pole decreased proportionally to the increase in the height of the animal pole and, in the surface of the polar body, the intensity became 0.5 compared with that of the control cortex. A similar deficiency in the cortex at the bulge region was reported during polar body formation using freshwater oligochaete and surf clam oocytes by electron microscopy and fluorescence microscopy (Shimizu, 1981a, 1981b, 1990: Pielak *et al*., 2004; Pielak *et al*., 2005). According to the diameter ratio of a polar body to an oocyte, the fluorescence intensity must be 0.07 if the surface force is generated simply by the interaction of actin and myosin (see Hamaguchi and Hiramoto, 1978). The thickness of the cortex, which in this study is estimated to be 1.4 μm from the fluorescence image of the oocyte, might result in overestimation of the actin amount in the cortex. Furthermore, the fluorescence intensity in the region near the mitotic apparatus was larger than that of the surrounding cytoplasm (see Figs. 1, 2, and 7), although it is not clear whether this was due to the presence of actin filaments in the mitotic apparatus or the transparency of the mitotic apparatus compared with the surrounding cytoplasm (Fig. 3). This excessive fluorescence in the region near the mitotic apparatus might also result in overestimation of the actin amount in the cortex. This discrepancy between the values of 0.5 and 0.07 will be diminished after future analysis such as a quantitative investigation of actin amounts in the isolated cortices instead of the investigation of digital dissection of the cortex from the image of the whole oocyte.

Actin filaments increased at the base of the bulge shortly after the beginning of the bulge formation, and then the base of the bulge became a furrow. In the division furrow, actin filaments accumulated to 1.8-fold of those in the reference cortex. Actin accumulation in the division furrow has been reported frequently including polar body formation using fluorescent phallotoxins (Strome, 1986; Yonemura and Kinoshita, 1986; Cao and Wang, 1990; Shimizu, 1990; Mabuchi, 1994; Li *et al*., 1997; Crawford *et al*., 1998; Satoh and Hamaguchi, 2000; Pielak *et al*., 2004, 2005) after the contractile ring was described in the division furrow by Schroeder (1968, 1970, 1972). Therefore, actin distribution

from the animal pole to the equatorial region of the oocyte is minimal at the pole, increases to maximal at the base of the bulge, and then decreases gradually to a constant value. In other words, bulge formation and furrow formation are caused by spatially different mechanisms.

Mechanism of polar body formation

Schematic representation of actin distribution in the cortex and morphological change in the oocyte near the animal pole during polar body formation is shown in Fig. 12. The present study provides evidence of two events, i.e., the decrease in cortical actin at the animal pole which is initial and essential to bulging, and the increase in cortical actin at the region adjacent to the animal pole, which results in contractile ring formation, and is also essential to cytokinesis. Dan (1963) discussed that it is difficult to explain unequal division either by a relaxation theory or by a contractile ring theory. During polar body formation, polar relaxation was suggested according to polar weakening (Wolpert, 1960; Hamaguchi and Hiramoto, 1978; Ohtsubo and Hiramoto, 1985). Actin deficiency in the polar region may be a molecular basis for polar weakening. Therefore, during unequal division, the actin filaments and the resultant generated forces decrease near the peripheral centrosome of the mitotic apparatus, which induces the cortex at the animal polar region to bulge due to the contraction of the cortex other than the animal pole. Thus, the different distances from the two centrosomes to the base of the bulge become equal after the mitotic apparatus, which is attached to the animal polar cortex (Hamaguchi, 2001), moves into the bulge. Although Hiramoto and colleagues (1978, 1985) suggested that polar weakening would be induced by the contraction of the contractile ring which had formed before bulging, polar weakening is the initial phenomenon or the phenomenon preceding contractile ring formation.

In contrast, the actin filaments and the resultant generated forces increase at the base of the bulge, which induces a contractile ring. Although a bulge did not form in the case of polar body inhibition, a contractile ring-like structure was induced at different distances from the two centrosomes of the mitotic apparatus. In other words, the mitotic apparatus, which attaches to the animal polar cortex, would induce actin deficiency at the animal pole as well as actin accumulation at the cortex slightly distant from the animal pole during anaphase.

Rappaport and Rappaport (1985) investigated polar body formation in various experiments using starfish and suggested that the bulge at polar body formation may not result from local surface weakening but from regional cytoskeletal activity. In the present study, among the cytoskeleton, actin distribution was investigated, and actin is deficient in the cortex of the bulge at the presumptive polar body region. We also investigated microtubule distribution during polar body formation and found that microtubules are richer near the peripheral aster than those near the inner aster (Satoh *et al*., 1994, 1996) and induced an ectopic polar body by means of displacing the mitotic apparatus (Hamaguchi, 2001), which suggests that the role of the microtubules in the mitotic apparatus is important for polar body formation. Pielak *et al*. (2004, 2005) suggested that peripheral aster spreading may be related to polar body contractile ring formation. Schaerer-Brodbeck and Riezman (2000) discussed the interdependence of filamentous actin and microtubules during asymmetric cell division. The role of these microtubules during polar body formation is a problem for the future.

Acknowledgements. We are deeply grateful for material supply to the staff of the Research Center for Marine Biology of Tohoku University, the staff of Marine and Coastal Research Center of Ochanomizu University, and Prof. S. Ikegami of Hiroshima University. This study was supported by Grants-in-Aid for Scientific Research from the Japan Ministry of Education, Culture, Sports, Science and Technology (Nos. 10213203 and 12680687).

References

Byers, H.R. and Fujiwara, K. 1982. Stress fibers in cells *in situ*: immunofluorescence visualization with antiactin antimyosin, and anti-alpha-actinin. *J. Cell Biol.*, **93**: 804–811.

Cao, L.G. and Wang, Y.L. 1990. Mechanism of the formation of contractile ring in dividing cultured animal cells. I. Recruitment of preexisting actin filaments into the cleavage furrow. *J. Cell Biol.*, **110**: 1089–1095.

Crawford, J.M., Harden, N., Leung, T., Lim, L., and Kiehart, D.P. 1998. Cellularization in *Drosophila melanogaster* is disrupted by the inhibition of rho activity and the activation of cdc42 function. *Dev. Biol.*, **204**: 151–164.

Dan, K. 1963. Force of cleavage of the dividing sea urchin egg. *Symp. Int. Soc. Cell Biol.*, **2**: 261–276.

Hamaguchi, M.S. and Hiramoto, Y. 1978. Protoplasmic movement during polar-body formation in starfish oocytes. *Exp. Cell Res.*, **112**: 55–62.

Hamaguchi, Y. 2001. Displacement of the mitotic apparatus which induces ectopic polar body formation or parthenogenetic cleavage in starfish oocytes. *Dev. Biol.*, **239**: 364–375.

Hamaguchi, Y. and Mabuchi, I. 1982. Effects of phalloidin microinjection and localization of fluorescein-labeled phalloidin in living sand dollar eggs. *Cell Motil.*, **2**: 103–113.

Hamaguchi, Y. and Mabuchi, I. 1988. Accumulation of fluorescently labeled actin in the cortical layer in sea urchin eggs after fertilization. *Cell Motil. Cytoskel.*, **9**: 153–163.

Heil-Chapdelaine, R.A. and Otto, J.J. 1996. Characterization of changes in F-actin during maturation of starfish oocytes. *Dev. Biol.*, **117**: 204–216.

Kanatani, H. 1969. Induction of spawning and oocyte maturation by 1-methyladenine in starfishes. *Exp. Cell Res.*, **57**: 333–337.

Li, F., Wang, X., Bunger, P.C., and Gerdes, A.M. 1997. Formation of binucleated cardiac myocytes in rat heart: I. Role of actin-myosin contractile ring. *J. Mol. Cell Cardiol.*, **29**: 1541–1551.

Longo, F.J. 1972. The effects of cytochalasin B on the events of fertilization in the surf clam, *Spisula solidissima*. I. Polar body formation. *J. Exp. Zool.*, **182**: 321–344.

Mabuchi, I. 1994. Cleavage furrow: Timing of emergence of contractile ring actin filaments and establishment of the contractile ring by filament bundling in sea urchin eggs. *J. Cell Sci.*, **107**: 1853–1862.

Ohtsubo, M. and Hiramoto, Y. 1985. Regional difference in mechanical properties of the cell surface in dividing echinoderm eggs. *Dev. Growth*

Differ., **27**: 371–383.

Pielak, R.M., Gaysinskaya, V.A., and Cohen, W.D. 2004. Formation and function of the polar body contractile ring in *Spisula*. *Dev. Biol.*, **269**: 421–432.

Pielak, R.M., Hawkins, C., Pyie, A., Bautista, J., Lee, K., and Cohen, W.D. 2005. Polar body formation in *Spisula* oocytes: Function of the peripheral aster. *Biol. Bull.*, **209**: 21–30.

Rappaport, R. 1961. Experiments concerning the cleavage stimulus in sand dollar eggs. *J. Exp. Zool.*, **148**: 81–89.

Rappaport, R. and Rappaport, B.N. 1985. Experimental analysis of polar body formation in starfish eggs. *J. Exp. Zool.*, **235**: 87–103.

Robinson, D.N., Cavet, G., Warrick, H.M., and Spudich, J.A. 2002. Quantitation of the distribution and flux of myosin-II during cytokinesis. *BMC Cell Biol.*, **3**: 4–15.

Saiki, T. and Hamaguchi, Y. 1998. Aster forming abilities of the egg, polar body, and sperm centrosomes in early starfish development. *Dev. Biol.*, **203**: 62–74.

Satoh, S.K. and Hamaguchi, Y. 2000. Quantitative analysis of cortical actin filaments in dividing sea urchin eggs. *Bioimages*, **8**: 105–111.

Satoh, S.K., Oka, M.T., and Hamaguchi, Y. 1994. Asymmetry in the mitotic spindle induced by the attachment to the cell surface during maturation in the starfish oocyte. *Dev. Growth Differ.*, **36**: 557–565.

Satoh, S.K., Satoh, R., and Hamaguchi, Y. 1996. Quantitative analysis of asymmetry of the mitotic apparatus during polar body formation in the starfish oocyte. *Bioimages*, **4**: 79–93.

Schaerer-Brodbeck, C. and Riezman, H. 2000. Interdependence of filamentous actin and microtubules for asymmetric cell division. *Biol. Chem.*, **381**: 815–825.

Schroeder, T.E. 1968. Cytokinesis: Filaments in the cleavage furrow. *Exp. Cell Res.*, **53**: 272–276.

Schroeder, T.E. 1970. The contractile ring. I. Fine structure of dividing mammalian (HeLa) cells and the effects of cytochalasin B. *Z. Zellenforsch. Mikrosk. Anat.*, **109**: 431–449.

Schroeder, T.E. 1972. The contractile ring. II. Determining its brief existence, volumetric changes, and vital role in cleaving *Arbacia* eggs. *J. Cell Biol.*, **53**: 419–434.

Shimizu, T. 1981a. Cortical differentiation of the animal pole during maturation division in fertilized eggs of *Tubifex* (Annelida, Oligochaeta). I. Meiotic apparatus formation. *Dev. Biol.*, **85**: 65–76.

Shimizu, T. 1981b. Cortical differentiation of the animal pole during maturation division in fertilized eggs of *Tubifex* (Annelida, Oligochaeta). II. Polar body formation. *Dev. Biol.*, **85**: 77–88.

Shimizu, T. 1990. Polar body formation in *Tubifex* eggs. *Ann. New York Acad. Sci.*, **582**: 260–272.

Shirai, H. and Kanatani, H. 1980. Effect of local application of 1-methyladenine on the site of polar body formation in starfish oocyte. *Dev. Growth Differ.*, **22**: 555–560.

Strome, S. 1986. Fluorescence visualization of the distribution of microfilaments in gonads and early embryos of the nematode Caenorhabditis elegans. *J. Cell Biol.*, **103**: 2241–2252.

Wolpert, L. 1960. The mechanics and mechanism of cleavage. *Int. Rev. Cytol.*, **10**: 163–216.

Yonemura, S. and Kinoshita, S. 1986. Actin filament organization in the sand dollar egg cortex. *Dev. Biol.*, **115**: 171–183.

Yumura, S. and Fukui, Y. 1998. Spatiotemporal dynamics of actin concentration during cytokinesis and locomotion in Dictyostelium. *J. Cell Sci.*, **111**: 2097–2108.

(Received for publication, November 21, 2006 and accepted March 6, 2007)